

# Variational Quantum Support Vector Machine based on $\Gamma$ matrix expansion and Variational Universal-Quantum-State Generator

Motohiko Ezawa

*Department of Applied Physics, University of Tokyo, Hongo 7-3-1, 113-8656, Japan*

We analyze a binary classification problem by using a support vector machine based on variational quantum-circuit model. We propose to solve a linear equation of the support vector machine by using a  $\Gamma$  matrix expansion. In addition, it is shown that an arbitrary quantum state is prepared by optimizing a universal quantum circuit representing an arbitrary  $U(2^N)$  based on the steepest descent method. It may be a quantum generalization of Field-Programmable-Gate Array (FPGA).

## Introduction

Quantum computation is a hottest topic in contemporary physics<sup>1-3</sup>. An efficient application of quantum computations is machine learning, which is called quantum machine learning<sup>4-15</sup>. A support vector machine is one of the most fundamental algorithms for machine learning<sup>16-18</sup>, which classifies data into two classes by a hyperplane. The optimal hyperplane is determined by an associated linear equation  $F|\psi_{\text{in}}\rangle = |\psi_{\text{out}}\rangle$ , where  $F$  and  $|\psi_{\text{out}}\rangle$  are given. A quantum support vector machine solves this linear equation by a quantum computer<sup>10,13,19</sup>. Usually, the linear equation is solved by the Harrow-Hassidim-Lloyd (HHL) algorithm<sup>20</sup>. However, this algorithm requires many quantum gates. Thus, the HHL algorithm is hard to be executed by using a near-term quantum computer. Actually, this algorithm has experimentally been verified only for two and three qubits<sup>21-23</sup>. In addition, it requires a unitary operator to execute  $e^{iFt}$ , which is quite hard to be implemented.

The number of qubits in current quantum computers is restricted. Variational quantum algorithms are appropriate for these small-qubit quantum computers, which use both quantum computers and classical computers. Various methods have been proposed such as Quantum Approximate Optimization Algorithm (QAOA)<sup>24</sup>, variational eigenvalue solver<sup>25</sup>, quantum circuit learning<sup>26</sup> and quantum linear solver<sup>27,28</sup>. We use wave functions with variational parameters in QAOA, which are optimized by minimizing the expectation value of the Hamiltonian. A quantum circuit has variational parameters in quantum circuit learning<sup>26</sup>, which are optimized by minimizing a certain cost function. A quantum linear solver solves a linear equation by variational ansatz<sup>27,28</sup>. The simplest method of the optimization is a steepest-descent method.

In this paper, we present a variational method for a quantum support vector machine by solving an associated linear equation based on variational quantum circuit learning. We propose a method to expand the matrix  $F$  by the  $\Gamma$  matrices, which gives simple quantum circuits. We also propose a variational method to construct an arbitrary state by using a universal quantum circuit to represent an arbitrary unitary matrix  $U(2^N)$ . We prepare various internal parameters for a universal quantum circuit, which we optimize by minimizing a certain cost function. Our circuit is capable to determine the unitary transformation  $U$  satisfying  $U|\psi_{\text{initial}}\rangle = |\psi_{\text{final}}\rangle$  with arbitrary given states  $|\psi_{\text{initial}}\rangle$  and  $|\psi_{\text{final}}\rangle$ . It will be a quantum generalization of field-programmable-gate array (FPGA), which may execute arbitrary outputs with arbitrary inputs.

## Results

### Support vector machine.

A support vector machine (SVM) is a computer algorithm that learns by examples to assign labels to objects. It is a typical method to solve a binary-classification problem<sup>16</sup>. A simplest example reads as follows. Suppose that there are red and blue points whose distributions are almost separated into two dimensions. We classify these data points into two classes by a line, as illustrated in Fig.1.

In general,  $M$  data points are spattered in  $D$  dimensions, which we denote  $\mathbf{x}_j$ , where  $1 \leq j \leq M$ . The problem is to determine a hyperplane,

$$\boldsymbol{\omega} \cdot \mathbf{x} + \omega_0 = 0, \quad (1)$$

separating data into two classes with the use of a support vector machine. We set

$$\boldsymbol{\omega} \cdot \mathbf{x} + \omega_0 > 0 \quad (2)$$

for red points and

$$\boldsymbol{\omega} \cdot \mathbf{x} + \omega_0 < 0 \quad (3)$$

for blue points. These conditions are implemented by introducing a function

$$f(\mathbf{x}) = \text{sgn}(\boldsymbol{\omega} \cdot \mathbf{x} + \omega_0), \quad (4)$$

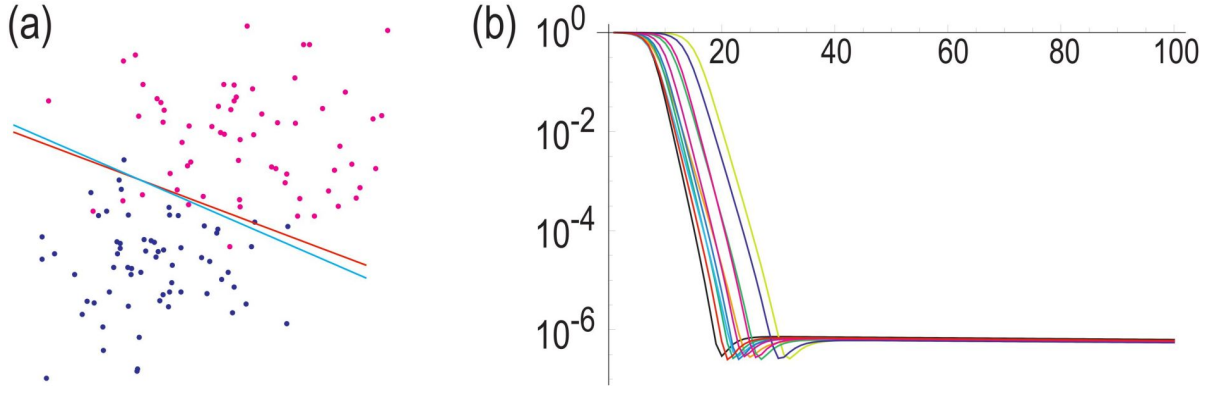


FIG. 1: (a) Binary classification of red and blue points based on a quantum support vector machine with soft margin. A magenta (cyan) line obtained by an exact solution (variational method). (b) Evolution of the cost function. The vertical axis is the  $\log_{10} E_{\text{cost}}$ . The horizontal axis is the variational step number. We have used  $r = 2$ ,  $\xi_1 = 0.001$  and  $\xi_2 = 0.0005$  and  $\gamma = 1$ . We have run simulations ten times.

which assigns  $f(\mathbf{x}) = 1$  to red points and  $f(\mathbf{x}) = -1$  to blue points. In order to determine  $\omega_0$  and  $\omega$  for a given set of data  $\mathbf{x}_j$ , we introduce real numbers  $\alpha_j$  by

$$\omega = \sum_{j=1}^M \alpha_j \mathbf{x}_j. \quad (5)$$

A support vector machine enables us to determine  $\omega_0$  and  $\alpha_j$  by solving the linear equation

$$F \begin{pmatrix} \omega_0 \\ \alpha_1 \\ \vdots \\ \alpha_M \end{pmatrix} = \begin{pmatrix} 0 \\ y_1 \\ \vdots \\ y_M \end{pmatrix}, \quad (6)$$

where  $y_i = f(x_i) = \pm 1$ , and  $F$  is a  $(M+1) \times (M+1)$  matrix given by

$$F = \begin{pmatrix} 0 & 1 & \cdots & 1 \\ 1 & & & \\ \vdots & & K + I_M/\gamma & \\ 1 & & & \end{pmatrix}. \quad (7)$$

Here,

$$K_{ij} = \mathbf{x}_i \cdot \mathbf{x}_j, \quad (8)$$

is a Kernel matrix, and  $\gamma$  is a certain fixed constant which assures the existence of the solution of the linear equation (6) even when the red and blue points are slightly inseparable. Note that  $\gamma \rightarrow \infty$  corresponds to the hard margin condition. Details of the derivation of Eq.(6) are given in Method A.

#### Quantum linear solver based on $\Gamma$ matrix expansion.

We solve the linear equation (6) by a quantum computer. In general, we solve a linear equation

$$F |\psi_{\text{in}}\rangle = c |\psi_{\text{out}}\rangle, \quad (9)$$

for an arbitrary given non-unitary matrix  $F$  and an arbitrary given state  $|\psi_{\text{out}}\rangle$ . Here, the coefficient  $c$  is introduced to preserve the norm of the state, and it is given by

$$c = \sqrt{\langle \psi_{\text{in}} | F^\dagger F | \psi_{\text{in}} \rangle}. \quad (10)$$

The HHL algorithm<sup>20</sup> is a most famous algorithm to solve this linear equation by a quantum computer. We first construct a Hermitian matrix by

$$H = \begin{pmatrix} 0 & F \\ F^\dagger & 0 \end{pmatrix}. \quad (11)$$

Then, a unitary matrix associated with  $F$  is uniquely obtained by  $e^{iHt}$ . Nevertheless, it requires many quantum gates. In addition, it is a nontrivial problem to implement  $e^{iHt}$ .

Recently, variational methods have been proposed<sup>27</sup> to solve the linear equation (9). In one of the methods, the matrix  $F$  is expanded in terms of some unitary matrices  $U_j$  as

$$F = \sum_{j=0}^{2^N-1} c_j U_j. \quad (12)$$

In general, a complicated quantum circuit is necessary to determine the coefficient  $c_j$ .

We start with a trial state  $|\tilde{\psi}_{\text{in}}\rangle$  to determine the state  $|\psi_{\text{in}}\rangle$ . Application of each unitary matrix to this state is efficiently done by a quantum computer,  $U_j|\tilde{\psi}_{\text{in}}\rangle = |\tilde{\psi}_{\text{out}}^{(j)}\rangle$ , and we obtain

$$F|\tilde{\psi}_{\text{in}}\rangle = \sum_{j=0}^{2^N-1} c_j U_j|\tilde{\psi}_{\text{in}}\rangle = \sum_{j=0}^{2^N-1} c_j |\tilde{\psi}_{\text{out}}^{(j)}\rangle \equiv c|\tilde{\psi}_{\text{out}}\rangle, \quad (13)$$

where  $|\tilde{\psi}_{\text{out}}\rangle$  is an approximation of the given state  $|\psi_{\text{out}}\rangle$ . We tune a trial state  $|\tilde{\psi}_{\text{in}}\rangle$  by a variational method so as to minimize the cost function<sup>27</sup>

$$E_{\text{cost}} \equiv 1 - \left| \langle \tilde{\psi}_{\text{out}} | \psi_{\text{out}} \rangle \right|^2, \quad (14)$$

which measures the similarity between the approximate state  $|\tilde{\psi}_{\text{out}}\rangle$  and the state  $|\psi_{\text{out}}\rangle$  in (9). We have  $0 \leq E_{\text{cost}} \leq 1$ , where  $E_{\text{cost}} = 0$  for the exact solution. The merit of this cost function is that the inner product is naturally calculated by a quantum computer.

Let the dimension of the matrix  $F$  be  $2^N$ . It is enough to use  $N$  satisfying  $2^{N-1} < D \leq 2^N$  without loss of generality by adding trivial  $2^N - D$  components to the linear equation. We propose to expand the matrix  $F$  by the gamma matrices  $\Gamma_j$  as

$$F = \sum_{j=0}^{2^N-1} c_j \Gamma_j, \quad (15)$$

with

$$\Gamma_j = \bigotimes_{\beta=1}^N \sigma_{\alpha}^{(\beta)}, \quad (16)$$

where  $\alpha = 0, x, y$  and  $z$ .

The merit of our method is that it is straightforward to determine  $c_j$  by the well-known formula

$$c_j = \text{Tr}[\Gamma_j F]. \quad (17)$$

In order to construct a quantum circuit to calculate  $c_j$ , we express the matrix  $F$  by column vectors as

$$F = \{|f_0\rangle, \dots, |f_{2^N-1}\rangle\}. \quad (18)$$

We have  $(|f_{q-1}\rangle)_p = F_{pq}$ , where subscript  $p$  denotes the  $p$ -th component of  $|f_{q-1}\rangle$ . Then  $c_j$  is given by

$$c_j = \sum_{q=0}^{2^N-1} (\Gamma_j |f_q\rangle)_q = \sum_{q=0}^{2^N-1} \langle q | \Gamma_j | f_q \rangle, \quad (19)$$

where the subscript  $q$  denotes the  $(q+1)$ -th component of  $\Gamma_j |f_q\rangle$ . We have introduced a notation  $|q\rangle \equiv |n_1 n_2 \dots n_N\rangle$  with  $n_i = 0, 1$ , where  $q$  is the decimal representation of the binary number  $n_1 n_2 \dots n_N$ . See explicit examples for one and two qubits in Method B.

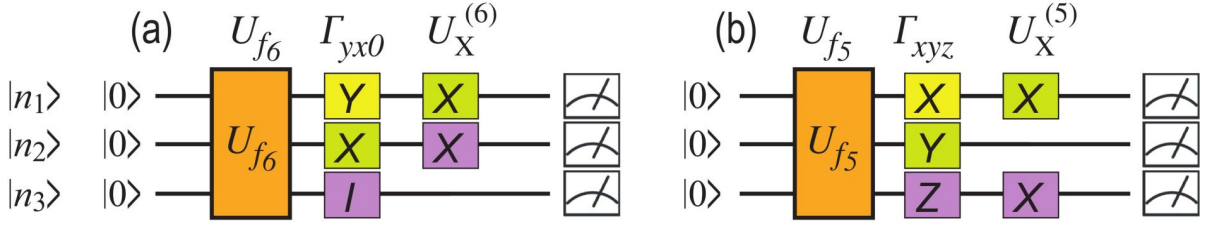


FIG. 2: Quantum circuits determining  $c_j$ . We show an example with (a)  $\Gamma_{yx0} = \sigma_y \otimes \sigma_x \otimes \sigma_0$ .  $U_X^{(6)} |0\rangle\rangle = \sigma_x^{(1)} \sigma_x^{(2)} |000\rangle = |110\rangle = |6\rangle\rangle$  and (b)  $\Gamma_{xyz} = \sigma_x \otimes \sigma_y \otimes \sigma_z$ .  $U_X^{(5)} |0\rangle\rangle = \sigma_x^{(1)} \sigma_x^{(3)} |000\rangle = |101\rangle = |5\rangle\rangle$ .

The state  $|q\rangle\rangle \equiv |n_1 n_2 \dots n_N\rangle$  is generated as follows. We prepare the NOT gates  $\sigma_x^{(i)}$  for the  $i$ -th qubit if  $n_i = 1$ . Using all these NOT gates we define

$$U_X^{(q)} = \bigotimes_{n_i=1} \sigma_x^{(i)}. \quad (20)$$

We act it on the initial state  $|0\rangle\rangle$  and obtain

$$U_X^{(q)} |0\rangle\rangle = |q\rangle\rangle. \quad (21)$$

Next, we construct a unitary gate  $U_{f_q}$  generating  $|f_q\rangle$ ,

$$U_{f_q} |0\rangle\rangle = |f_q\rangle. \quad (22)$$

We will discuss how to prepare  $U_{f_q}$  by a quantum circuit soon later; See Eq.(28). By using these operators,  $c_j$  is expressed as

$$c_j = \sum_{q=0}^{2^N-1} \langle\langle 0 | U_X^{(q)} \Gamma_j U_{f_q} | 0 \rangle\rangle, \quad (23)$$

which can be executed by a quantum computer. We show explicit examples in Fig.2.

Once we have  $c_j$ , the final state is obtained by applying  $\Gamma_j$  to  $|\tilde{\psi}_{\text{in}}\rangle$  and taking sum over  $j$ , which leads to

$$|\tilde{\psi}_{\text{out}}\rangle = F|\tilde{\psi}_{\text{in}}\rangle = \sum_{j=0}^{2^N-1} c_j \Gamma_j |\tilde{\psi}_{\text{in}}\rangle. \quad (24)$$

The implementation of the  $\Gamma$  matrix is straightforward in quantum circuit, because the  $\Gamma$  matrix is composed of the Pauli sigma matrices, as shown in Fig.2.

We may use the steepest descent method to find an optimal trial state  $|\tilde{\psi}_{\text{in}}\rangle$  closest to the state  $|\psi_{\text{in}}\rangle$ . We calculate the difference of the cost function  $\Delta E_{\text{cost}}$  when we slightly change the trial state  $|\tilde{\psi}_{\text{in}}(t)\rangle$  at step  $t$  by the amount of  $\Delta|\tilde{\psi}_{\text{in}}(t)\rangle$  as

$$\Delta E_{\text{cost}} \equiv E_{\text{cost}}(|\tilde{\psi}_{\text{in}}(t)\rangle + \Delta|\tilde{\psi}_{\text{in}}(t)\rangle) - E_{\text{cost}}(|\tilde{\psi}_{\text{in}}(t)\rangle) \simeq \frac{\Delta E_{\text{cost}}}{\Delta|\tilde{\psi}_{\text{in}}(t)\rangle} \Delta|\tilde{\psi}_{\text{in}}(t)\rangle. \quad (25)$$

We explain how to construct  $|\tilde{\psi}_{\text{in}}(t)\rangle$  by a quantum circuit soon later; See Eq.(28). Then, we renew the state as

$$|\tilde{\psi}_{\text{in}}(t)\rangle \rightarrow |\tilde{\psi}_{\text{in}}(t)\rangle - \eta_t \frac{\Delta E_{\text{cost}}}{\Delta|\tilde{\psi}_{\text{in}}(t)\rangle} \Delta|\tilde{\psi}_{\text{in}}(t)\rangle, \quad (26)$$

where we use an exponential function for  $\eta_t$ ,

$$\eta_t = \xi_1 e^{-\xi_2 t}. \quad (27)$$

We choose appropriate constants  $\xi_1$  and  $\xi_2$  for an efficient search of the optimal solution, whose explicit examples are given in the caption of Fig.2. We stop the renewal of the variational step when the difference  $\Delta|\tilde{\psi}_{\text{in}}(t)\rangle$  becomes sufficiently small, which gives the optimal state of the linear equation (9).

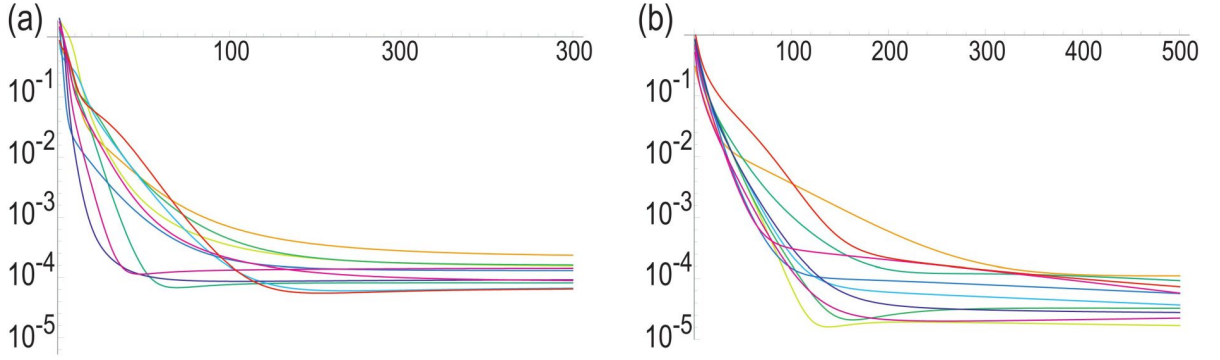


FIG. 3: Evolution of the cost function for (a) two qubits and (b) three qubits. The vertical axis is the  $\log_{10} E_{\text{cost}}$ . The horizontal axis is the number of variational steps. We use  $c_1 = 0.005$  and  $c_2 = 0.005$  for both the two- and three-qubit universal quantum circuits. We prepare random initial and final states, where we have run simulations ten times.

### Variational universal-quantum-state generator.

In order to construct the trial state  $|\tilde{\psi}_{\text{in}}(t)\rangle$ , it is necessary to prepare an arbitrary state  $|\psi\rangle$  by a quantum circuit. Alternatively, we need such a unitary transformation  $U$  that

$$U |0\rangle\rangle = |\psi\rangle. \quad (28)$$

It is known that any unitary transformation is done by a sequential application of the Hadamard, the  $\pi/4$  phase-shift and the CNOT gates<sup>29,30</sup>. Indeed, an arbitrary unitary matrix is decomposable into a sequential application of quantum gates<sup>29,30</sup>, each of which is constructed as a universal quantum circuit systematically<sup>31–36</sup>. Universal quantum circuits have so far been demonstrated experimentally for two and three qubits<sup>37–40</sup>.

We may use a variational method to construct  $U$  satisfying Eq.(28). Quantum circuit learning is a variational method<sup>26</sup>, where angle variables  $\theta_i$  are used as variational parameters in a quantum circuit  $U$ , and the cost function is optimized by tuning  $\theta_i$ . We propose to use a quantum circuit learning for a universal quantum circuit. We show that an arbitrary state  $|\psi(\theta_i)\rangle$  can be generated by tuning  $U(\theta_i)$  starting from the initial state  $|0\rangle\rangle$  as

$$U(\theta_i) |0\rangle\rangle = |\psi(\theta_i)\rangle. \quad (29)$$

We adjust  $\theta_i$  by minimizing the cost function

$$E_{\text{cost}}(\theta_i) \equiv 1 - |\langle\psi(\theta_i)|\psi\rangle|^2, \quad (30)$$

which is the same as that of the variational quantum support vector machine. We present explicit examples of universal quantum circuits for one, two and three qubits in Method C.

### Quantum Field-Programmable-Gate Array.

We next consider a problem to find a unitary transformation  $U_{\text{ini-fin}}$  which maps an arbitrary initial state  $|\psi_{\text{initial}}\rangle$  to an arbitrary final state  $|\psi_{\text{final}}\rangle$ ,

$$U_{\text{ini-fin}} |\psi_{\text{initial}}\rangle = |\psi_{\text{final}}\rangle. \quad (31)$$

Since we can generate an arbitrary unitary matrix as in Eq.(28), it is possible to generate such matrices  $U_{\text{ini}}$  and  $U_{\text{fin}}$  that

$$U_{\text{ini}} |0\rangle\rangle = |\psi_{\text{initial}}\rangle, \quad U_{\text{fin}} |0\rangle\rangle = |\psi_{\text{final}}\rangle. \quad (32)$$

Then, Eq.(31) is solved as

$$U_{\text{fin}} = U_{\text{ini-fin}} U_{\text{ini}}, \quad (33)$$

since  $U_{\text{ini-fin}} |\psi_{\text{initial}}\rangle = U_{\text{ini-fin}} U_{\text{ini}} |0\rangle\rangle = |\psi_{\text{final}}\rangle = U_{\text{fin}} |0\rangle\rangle$ .

An FPGA is a classical integrated circuit, which can be programmable by a customer or a designer after manufacturing in a factory. An FPGA executes any classical algorithms. On the other hand, our variational universal quantum-state generator creates an arbitrary quantum state. We program by using the variational parameters  $\theta_i$ . In this sense, the above quantum circuit may be considered as a quantum generalization of FPGA, which is a quantum FPGA (q-FPGA).

We show explicitly how the cost function is renewed for each variational step in the case of two- and three-qubit universal quantum circuits in Fig.3, where we have generated the initial and the final states randomly. We optimize 15 parameters  $\theta_i$  for two-qubit universal quantum circuits and 82 parameters  $\theta_i$  for three-qubit universal quantum circuits. We find that  $U_{\text{ini-fin}}$  is well determined by variational method as in Fig.3.

### Variational quantum support vector machine.

We demonstrate a binary classification problem in two dimensions based on the support vector machine. We prepare a data set, where red points have a distribution around  $(r \cos \Theta, r \sin \Theta)$  with variance  $r$ , while blue points have a distribution around  $(-r \cos \Theta, -r \sin \Theta)$  with variance  $r$ . We assume the Gaussian normal distribution. We choose  $\Theta$  randomly. We note that there are some overlaps between the red and blue points, which is the soft margin model.

As an example, we show the distribution of red and blue points and the lines obtained by the variational method marked in cyan and by the direct solution of (6) marked in magenta in Fig.1. They agree well with one another, where both of the lines well separate red and blue points. We have prepared 31 red points and 32 blue points, and used six qubits.

## Discussion

We have proposed that the matrix  $F$  is efficiently inputted into a quantum computer by using the  $\Gamma$ -matrix expansion method. There are many ways to use a matrix in a quantum computer such as linear regression and principal component analysis. Our method will be applicable to these cases.

Although it is possible to obtain the exact solution for the linear equation by the HHL algorithm, it requires many gates. On the other hand, it is often hard to obtain the exact solution by variational methods since trial functions may be trapped to a local minimum. However, this problem is not serious for the machine learning problem because it is more important to obtain an approximate solution efficiently rather than an exact solution by using many gates. Indeed, our optimized hyperplane also well separates red and blue points as shown in Fig.1(a).

In order to classify  $M$  data, we need to prepare  $\log_2 M$  qubits. It is hard to execute a large number of data points by current quantum computers. Recently, it is shown that electric circuits may simulate universal quantum gates<sup>41–43</sup> based on the fact that the Kirchhoff law is rewritten in the form of the Schrödinger equation<sup>44</sup>. Our variational algorithm will be simulated by using them.

## Methods

### A: Support vector machine.

A support vector machine is an algorithm for supervised learning<sup>16–18</sup>. We first prepare a set of training data, where each point is marked either in red or blue. Then, we determine a hyperplane separating red and blue points. After learning, input data are classified into red or blue by comparing the input data with the hyperplane. The support vector machine maximizes a margin, which is a distance between the hyperplane and data points. If red and blue points are perfectly separated by the hyperplane, it is called a hard margin problem [Fig.4(a)]. Otherwise, it is called a soft margin problem [Fig.4(b)].

We minimize the distance  $d_j$  between a data point  $\mathbf{x}_j$  and the hyperplane given by

$$d_j = \frac{|\boldsymbol{\omega} \cdot \mathbf{x}_j + \omega_0|}{|\boldsymbol{\omega}|}. \quad (34)$$

We define support vectors  $\mathbf{x}$  as the closest points to the hyperplane. There is such a vector in each side of the hyperplane, as shown in Fig.4(a). This is the origin of the name of the support vector machine. Without loss of generality, we set

$$|\boldsymbol{\omega} \cdot \mathbf{x} + \omega_0| = 1 \quad (35)$$

for the support vectors, because the hyperplane is present at the equidistance of two closest data points and because it is possible to set the magnitude of  $|\boldsymbol{\omega} \cdot \mathbf{x} + \omega_0|$  to be 1 by scaling  $\boldsymbol{\omega}$  and  $\omega_0$ . Then, we maximize the distance

$$d = \frac{|\boldsymbol{\omega} \cdot \mathbf{x} + \omega_0|}{|\boldsymbol{\omega}|} = \frac{1}{|\boldsymbol{\omega}|}, \quad (36)$$

which is identical to minimize  $|\boldsymbol{\omega}|$ .

First, we consider the hard margin problem, where red and blue points are perfectly separable. All red points satisfy  $\boldsymbol{\omega} \cdot \mathbf{x}_j + \omega_0 > 1$  and all blue points satisfy  $\boldsymbol{\omega} \cdot \mathbf{x}_j + \omega_0 < -1$ . We introduce variables  $y_j$ , where  $y_j = 1$  for red points and  $y_j = -1$  for blue points. Using them, the condition is rewritten as

$$(\boldsymbol{\omega} \cdot \mathbf{x}_j + \omega_0) y_j \geq 1 \quad (37)$$

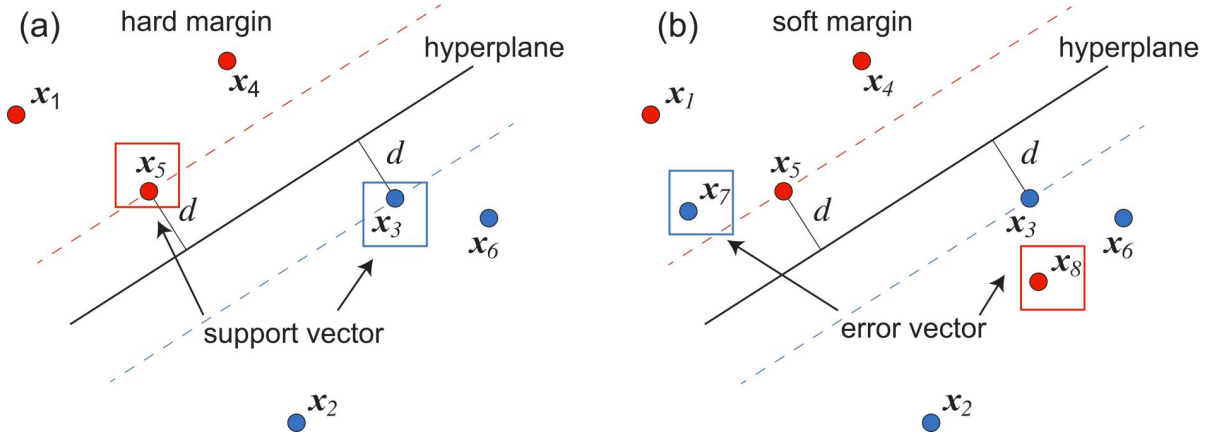


FIG. 4: Illustration of the hyperplane and the support vector. Two support vectors are marked by red and blue squares. (a) Hard margin where red and blue points are separated perfectly, and (b) soft margin where they are separated imperfectly.

for each  $j$ . The problem is reduced to find the minimum of  $|\omega|^2$  under the above inequalities. The optimization under inequality conditions is done by the Lagrange multiplier method with the Karush-Kuhn-Tucker condition<sup>45</sup>. It is expressed in terms of the Lagrangian as

$$L(\omega, \omega_0, \alpha) = \frac{1}{2} |\omega|^2 - \sum_j \beta_j [(\omega \cdot x_j + \omega_0) y_j - 1], \quad (38)$$

where  $\beta_j$  are Lagrange multipliers to ensure the constraints.

For the soft margin case, we cannot separate two classes exactly. In order to treat this case, we introduce slack variables  $\xi_j$  satisfying

$$(\omega \cdot x_j + \omega_0) y_j \geq 1 - \xi_j, \quad \xi_j \geq 0 \quad (39)$$

and redefine the cost function as

$$E_{\text{cost}} = \frac{1}{2} |\omega|^2 + \gamma \sum_{j=1}^M \xi_j^2. \quad (40)$$

Here,  $\gamma = \infty$  corresponds to the hard margin. The second term represents the penalty for some of data points to have crossed over the hyperplane. The Lagrangian is modified as

$$L(\omega, \omega_0, \xi_i, \beta) = \frac{1}{2} |\omega|^2 + \gamma \sum_{j=1}^M \xi_j^2 - \sum_{j=1}^M [(\omega \cdot x_j + \omega_0) \beta_j y_j - (1 - \xi_i)]. \quad (41)$$

The stationary points are determined by

$$\frac{\partial L}{\partial \omega} = \omega - \sum_{j=1}^M \beta_j y_j x_j = 0, \quad (42)$$

$$\frac{\partial L}{\partial \omega_0} = - \sum_{j=1}^M \beta_j y_j = 0, \quad (43)$$

$$\frac{\partial L}{\partial \xi_j} = \gamma \xi_j - \beta_j = 0, \quad (44)$$

$$\frac{\partial L}{\partial \beta_j} = (\omega \cdot x_j + \omega_0) y_j - (1 - \xi_i) = 0. \quad (45)$$

We may solve these equations to determine  $\omega$  and  $\nu_j$  as

$$\omega = \sum_{j=1}^M \beta_j y_j x_j, \quad (46)$$

from (42), and

$$\xi_j = \beta_j/\gamma \quad (47)$$

from (44). Inserting them into (45), we find

$$y_j \sum_{i=1}^M (\beta_i y_i \mathbf{x}_i \cdot \mathbf{x}_j + \omega_0) - (1 - \beta_j/\gamma) = 0. \quad (48)$$

Since  $y_j^2 = 1$ , it is rewritten as

$$\omega_0 + \sum_{i=1}^M (\mathbf{x}_i \cdot \mathbf{x}_j + \delta_{ij}/\gamma) \beta_i y_i = y_j. \quad (49)$$

Since  $\beta_j$  appears always in a pair with  $y_j$ , we introduce a new variable defined by

$$\alpha_j = \beta_j y_j, \quad (50)$$

and we define the Kernel matrix  $K_{ij}$  as

$$K_{ij} = \mathbf{x}_i \cdot \mathbf{x}_j. \quad (51)$$

Then,  $\omega_0$  and  $\alpha_j$  are obtained by solving linear equations

$$\sum_{i=1}^M \alpha_i = 0, \quad (52)$$

$$\omega_0 + \sum_{i=1}^M (\mathbf{x}_i \cdot \mathbf{x}_j + \delta_{ij}/\gamma) \alpha_i = y_j, \quad (53)$$

which are summarized as

$$\begin{pmatrix} 0 & 1 & \cdots & 1 \\ 1 & & & \\ \vdots & K + I_M/\gamma & & \\ 1 & & & \end{pmatrix} \begin{pmatrix} \omega_0 \\ \alpha_1 \\ \vdots \\ \alpha_M \end{pmatrix} = \begin{pmatrix} 0 \\ y_1 \\ \vdots \\ y_M \end{pmatrix}, \quad (54)$$

which is Eq.(6) in the main text. Finally,  $\omega$  is determined by

$$\omega = \sum_{j=1}^M \alpha_j \mathbf{x}_j. \quad (55)$$

Once the hyperplane is determined, we can classify new input data into red if

$$\omega \cdot \mathbf{x}_j + \omega_0 > 0 \quad (56)$$

and blue if

$$\omega \cdot \mathbf{x}_j + \omega_0 < 0. \quad (57)$$

Thus, we obtain the hyperplane for binary classification.

### B: $\Gamma$ matrix expansion.

We explicitly show how to calculate  $c_j$  in (17) based on the  $\Gamma$  matrix expansion for the one and two qubits.

#### One qubit:

We show an explicit example of the  $\Gamma$ -matrix expansion for one qubit. One qubit is represented by a  $2 \times 2$  matrix,

$$F = \begin{pmatrix} F_{11} & F_{12} \\ F_{21} & F_{22} \end{pmatrix}. \quad (58)$$



The column vectors are explicitly given by

$$|f_1\rangle = \begin{pmatrix} F_{11} \\ F_{21} \end{pmatrix} = F_{11} |0\rangle + F_{21} |1\rangle, \quad (59)$$

$$|f_2\rangle = \begin{pmatrix} F_{12} \\ F_{22} \end{pmatrix} = F_{12} |0\rangle + F_{22} |1\rangle. \quad (60)$$

The coefficient  $c_j$  in (17) is calculated as

$$c_j = \text{Tr}[\sigma_j F] = \langle 0|\sigma_j|f_1\rangle + \langle 1|\sigma_j|f_2\rangle = \sum_{p=0,1} \langle p|\sigma_j|f_p\rangle = \sum_{p=0,1} \langle 0|U_X^{(p)}\sigma_j U_{f_p}|0\rangle. \quad (61)$$

### Two qubits:

Next, we show an explicit example of the  $\Gamma$ -matrix expansion for two qubits. Two qubits are represented by a  $4 \times 4$  matrix,

$$F = \begin{pmatrix} F_{11} & F_{12} & F_{13} & F_{14} \\ F_{21} & F_{22} & F_{23} & F_{24} \\ F_{31} & F_{32} & F_{33} & F_{34} \\ F_{41} & F_{42} & F_{43} & F_{44} \end{pmatrix}. \quad (62)$$

The column vectors are explicitly given by

$$|f_1\rangle = \begin{pmatrix} F_{11} \\ F_{21} \\ F_{31} \\ F_{41} \end{pmatrix} = F_{11} |00\rangle + F_{21} |01\rangle + F_{31} |10\rangle + F_{41} |11\rangle, \quad (63)$$

$$|f_2\rangle = \begin{pmatrix} F_{12} \\ F_{22} \\ F_{32} \\ F_{42} \end{pmatrix} = F_{12} |00\rangle + F_{22} |01\rangle + F_{32} |10\rangle + F_{42} |11\rangle, \quad (64)$$

$$|f_3\rangle = \begin{pmatrix} F_{13} \\ F_{23} \\ F_{33} \\ F_{43} \end{pmatrix} = F_{13} |00\rangle + F_{23} |01\rangle + F_{33} |10\rangle + F_{43} |11\rangle, \quad (65)$$

$$|f_4\rangle = \begin{pmatrix} F_{14} \\ F_{24} \\ F_{34} \\ F_{44} \end{pmatrix} = F_{14} |00\rangle + F_{24} |01\rangle + F_{34} |10\rangle + F_{44} |11\rangle. \quad (66)$$

The coefficient  $c_j$  in (17) is calculated as

$$c_j = \text{Tr}[\Gamma_j F] = \langle 00|\Gamma_j|f_1\rangle + \langle 01|\Gamma_j|f_2\rangle + \langle 10|\Gamma_j|f_3\rangle + \langle 11|\Gamma_j|f_4\rangle = \sum_{p=0}^3 \langle p|\Gamma_j|f_p\rangle = \sum_{p=0}^3 \langle\langle 0|U_X^{(p)}\Gamma_j U_{f_p}|0\rangle\rangle. \quad (67)$$

### C: Universal quantum circuits.

Angle variables are used as variational parameters in a universal quantum circuit learning. We present examples for one, two and three qubits.

#### One-qubit universal quantum circuit:

The single-qubit rotation gates are defined by

$$R(\theta, \phi) = \exp[-i\theta(\sigma_x \cos \phi + \sigma_y \sin \phi)/2], \quad (68)$$

$$R_z(\phi_z) = \exp[-i\sigma_z \phi_z/2]. \quad (69)$$

The one-qubit universal quantum circuit is constructed as

$$U^{(1)}(\theta, \phi, \phi_z) = R(\theta, \phi) R_z(\phi_z) = \begin{pmatrix} e^{-i\phi_z/2} \cos \frac{\theta}{2} & -ie^{i(\phi_z/2-\phi)} \sin \frac{\theta}{2} \\ -ie^{-i(\phi_z/2-\phi)} \sin \frac{\theta}{2} & e^{i\phi_z/2} \cos \frac{\theta}{2} \end{pmatrix}. \quad (70)$$

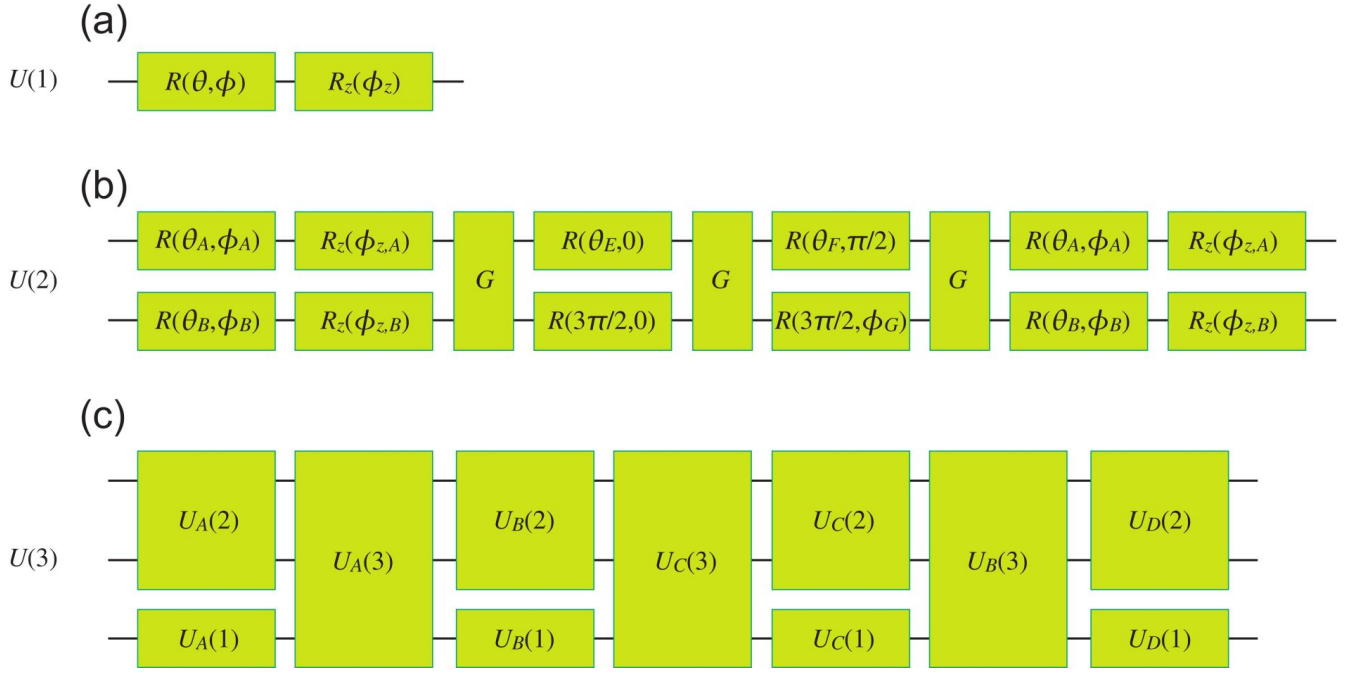


FIG. 5: Universal quantum circuits for (a) one, (b) two and (c) three qubits.

We show a quantum circuit in Fig.5(a). There are three variational parameters.

It is obvious that an arbitrary state is realized starting from the state  $|0\rangle$  as

$$U(1) \begin{pmatrix} 1 \\ 0 \end{pmatrix} = \begin{pmatrix} e^{-i\phi_z/2} \cos \frac{\theta}{2} \\ -ie^{-i(\phi_z/2-\phi)} \sin \frac{\theta}{2} \end{pmatrix}. \quad (71)$$

### Two-qubit universal quantum circuit:

The two-qubit universal quantum circuit is constructed as<sup>37</sup>

$$U(2) \equiv \left[ U^{(1)}(\theta_A, \phi_A, \phi_{z,A}) \otimes U^{(1)}(\theta_B, \phi_B, \phi_{z,B}) \right] U_G \left[ R(\theta_E, 0) \otimes R\left(\frac{3\pi}{2}, 0\right) \right] U_G \left[ R\left(\theta_F, \frac{\pi}{2}\right) \otimes R\left(\frac{3\pi}{2}, \theta_G\right) \right] U_G \left[ U^{(1)}(\theta_C, \phi_C, \phi_{z,C}) \otimes U^{(1)}(\theta_D, \phi_D, \phi_{z,D}) \right], \quad (72)$$

where the entangling two-qubit gate is defined by<sup>37</sup>

$$U_G = e^{-i\pi/4} \exp \left[ \frac{i\pi}{4} \sigma_z \otimes \sigma_z \right]. \quad (73)$$

The two-qubits universal quantum circuit contains 15 variational parameters. We show a quantum circuit in Fig.5(b).

### Three-qubit universal quantum circuit:

The three-qubit universal quantum circuit is constructed as

$$U(3) \equiv \left[ U_A^{(2)} \otimes U_A^{(1)} \right] U_A(3) \left[ U_B^{(2)} \otimes U_B^{(1)} \right] U_C(3) \left[ U_C^{(2)} \otimes U_C^{(1)} \right] U_B(3) \left[ U_D^{(2)} \otimes U_D^{(1)} \right], \quad (74)$$

where  $U_A^{(1)}$ ,  $U_B^{(1)}$ ,  $U_C^{(1)}$ , and  $U_D^{(1)}$  are one-qubit universal quantum circuits, while  $U_A^{(2)}$ ,  $U_B^{(2)}$ ,  $U_C^{(2)}$ , and  $U_D^{(2)}$  are two-qubit universal quantum circuit and

$$U_A(3) = \exp \left[ i \left( \theta_{xxz}^A \sigma_x \otimes \sigma_x \otimes \sigma_z + \theta_{yyz}^A \sigma_y \otimes \sigma_y \otimes \sigma_z + \theta_{zzz}^A \sigma_z \otimes \sigma_z \otimes \sigma_z \right) \right], \quad (75)$$

$$U_B(3) = \exp \left[ i \left( \theta_{xxz}^B \sigma_x \otimes \sigma_x \otimes \sigma_z + \theta_{yyz}^B \sigma_y \otimes \sigma_y \otimes \sigma_z + \theta_{zzz}^B \sigma_z \otimes \sigma_z \otimes \sigma_z \right) \right], \quad (76)$$

$$U_C(3) = \exp \left[ i \left( \theta_{xxx}^C \sigma_x \otimes \sigma_x \otimes \sigma_x + \theta_{yyx}^C \sigma_y \otimes \sigma_y \otimes \sigma_x + \theta_{zzx}^C \sigma_z \otimes \sigma_z \otimes \sigma_x + \theta_{00x}^C \sigma_0 \otimes \sigma_0 \otimes \sigma_x \right) \right]. \quad (77)$$

Explicit quantum circuits for  $U_A(3)$ ,  $U_B(3)$  and  $U_C(3)$  are shown in Ref.<sup>36</sup>. The three-qubits universal quantum circuit contains 82 variational parameters. We show a quantum circuit in Fig.5(c).

### Multi-qubit universal quantum circuit:

General multi-qubit universal quantum circuit is constructed in Ref.<sup>33</sup>. The minimum numbers of variational parameters are  $4^N - 1$  for  $N$ -qubit universal quantum circuits. However, we need more variational parameters in the currently known algorithm for  $N \geq 3$ .

- 
- <sup>1</sup> R. Feynman, Int. J. Theor. Phys. 21, 467 (1982).
  - <sup>2</sup> D. P. DiVincenzo, Science 270, 255 (1995).
  - <sup>3</sup> M. Nielsen and I. Chuang, Quantum Computation and Quantum Information, Cambridge University Press, 2016, p. 189; ISBN 978-1-107-00217-3.
  - <sup>4</sup> S. Lloyd, M. Mohseni and P. Rebentrost, arXiv:1307.0411
  - <sup>5</sup> M. Schuld, I. Sinayskiy, F. Petruccione, Contemporary Physics. 56, 172 (2014).
  - <sup>6</sup> P. Wittek, Quantum Machine Learning: What Quantum Computing Means to Data Mining Academic Press (2014)
  - <sup>7</sup> J. Biamonte, Nature. 549, 195 (2017).
  - <sup>8</sup> A. W. Harrow, A. Hassidim and S. Lloyd, Phys. Rev. Lett. 103 150502 (2009)
  - <sup>9</sup> N. Wiebe, D. Braun and S. Lloyd, Phys. Rev. Lett. 109, 050505 (2012)
  - <sup>10</sup> P. Rebentrost, M. Mohseni, S. Lloyd, Phys. Rev. Lett. 113, 130503 (2014)
  - <sup>11</sup> Z. Li, X. Liu, N. Xu and J. Du, Phys. Rev. Lett. 114, 140504 (2015).
  - <sup>12</sup> M. Schuld and N. Killoran, Phys. Rev. Lett. 122, 040504 (2019).
  - <sup>13</sup> V. Havlicek, A. D. Corcoles, K. Temme, A. W. Harrow, A. Kandala, J. M. Chow, J. M. Gambetta, Nature. vol. 567, pp. 209 (2019)
  - <sup>14</sup> I. Cong, S. Choi and M. D. Lukin, Nature Physics 15, 1273 (2019).
  - <sup>15</sup> L. Lamata, Mach. Learn.: Sci. Technol. 1, 033002 (2020).
  - <sup>16</sup> V. Vapnik and A. Lerner, Automation and Remote Control, 24, (1963)
  - <sup>17</sup> W. S. Noble, Nature Biotechnology 24, 1565 (2006)
  - <sup>18</sup> J. A. K. Suykens and J. Vandewalle, Neural Processing Letters 9, 293 (1999)
  - <sup>19</sup> L. Zhaokai, L. Xiaomei, X. Nanyang, D. jiangfeng, Phys. Rev. Lett. 114, 140504 (2015)
  - <sup>20</sup> A. W. Harrow, A. Hassidim, S. Lloyd, Phys. Rev. Lett. 15, 150502 (2009)
  - <sup>21</sup> X.-D. Cai, C. Weedbrook, Z.-E. Su, M.-C. Chen, Mile Gu, M.-J. Zhu, L. Li, N.-L. Liu, C.-Y. Lu, J.-W. Pan, Phys. Rev. Lett. 110, 230501 (2013)
  - <sup>22</sup> S. Barz, I. Kassal, M. Ringbauer, Y. O. Lipp, B. Dakic, A. Aspuru-Guzik, P. Walther, Scientific Reports 4,115 (2014)
  - <sup>23</sup> J. Pan, Y. Cao, X. Yao, Z. Li, C. Ju, X. Peng, S. Kais and J. Du, Phys. Rev. A 89, 022313 (2014)
  - <sup>24</sup> E. Farhi, J. Goldstone, S. Gutmann, MIT-CTP/4610
  - <sup>25</sup> A. Peruzzo, J. McClean, P. Shadbolt, M.-H. Yung, X.-Q. Zhou, P. J. Love, A. Aspuru-Guzik, J. L. O'Brien, Nature Communications, 5:4213, (2014)
  - <sup>26</sup> K. Mitarai, M. Negoro, M. Kitagawa and K. Fujii, Phys. Rev. A 98, 032309 (2018)
  - <sup>27</sup> C. Bravo-Prieto, R. LaRose, M. Cerezo, Y. Subasi, L. Cincio, P. J. Coles, LA-UR-19-29101
  - <sup>28</sup> X. Xu, J. Sun, S. Endo, Y. Li, S. C. Benjamin, X. Yuan, arXiv:1909.03898
  - <sup>29</sup> D. Deutsch, Proceedings of the Royal Society A. 400, 97 (1985)
  - <sup>30</sup> C. M. Dawson and M. A. Nielsen arXiv:quant-ph/0505030.
  - <sup>31</sup> B. Kraus and J.I. Cirac, Phys. Rev. A 63, 062309 (2001)
  - <sup>32</sup> G. Vidal, C. M. Dawson, Phys. Rev. A 69, 010301 (2004)
  - <sup>33</sup> M. Mottonen, J. J. Vartiainen, V. Bergholm, M. M. Salomaa, Phys. Rev. Lett. 93, 130502 (2004)
  - <sup>34</sup> V. V. Shende, I. L. Markov, S. S. Bullock, Physical Review A 69, 062321 (2004).
  - <sup>35</sup> F. Vatan and C. P. Williams, arXiv:quant-ph/0401178
  - <sup>36</sup> P. B. M. Sousa, R. V. Ramos, arXiv:quant-ph/0602174
  - <sup>37</sup> D. Hanneke, J. P. Home, J. D. Jost, J. M. Amini, D. Leibfried, D. J. Wineland, Nature Physics 6, 13 (2009)
  - <sup>38</sup> L. DiCarlo, J. M. Chow, J. M. Gambetta, Lev S. Bishop, B. R. Johnson, D. I. Schuster, J. Majer, A. Blais, L. Frunzio, S. M. Girvin, R. J. Schoelkopf, Nature 460, 240 (2009)
  - <sup>39</sup> X. Qiang, X. Zhou, J. Wang, C. M. Wilkes, T. Loke, S. O'Gara, L. Kling, G. D. Marshall, R. Santagati, T. C. Ralph, J. B. Wang, J. L. O'Brien, M. G. Thompson, J. C. F. Matthews, Nature Photonics 12, 534 (2018)
  - <sup>40</sup> T. Roy, S. Hazra, S. Kundu, M. Chand, M. P. Patankar and R. Vijay, Phys. Rev. Applied 14, 014072 (2020)
  - <sup>41</sup> M. Ezawa, Phys. Rev. Research 2, 023278 (2020).
  - <sup>42</sup> M. Ezawa, J. Phys. Soc. Jpn. 89, 124712 (2020)
  - <sup>43</sup> M. Ezawa, cond-mat/arXiv:2012.06124
  - <sup>44</sup> M. Ezawa, Phys. Rev. B 100, 165419 (2019).
  - <sup>45</sup> H. W. Kuhn and A. W. Tucker, Proceedings of 2nd Berkeley Symposium. Berkeley: University of California Press. pp. 481–492.

## **Acknowledgements**

The author is very much grateful to E. Saito and N. Nagaosa for helpful discussions on the subject. This work is supported by the Grants-in-Aid for Scientific Research from MEXT KAKENHI (Grants No. JP17K05490 and No. JP18H03676). This work is also supported by CREST, JST (JPMJCR16F1 and JPMJCR20T2).

## **Author contributions**

M.E. conceived the idea, performed the analysis, and wrote the manuscript.

## **Additional information**

**Competing financial and non-financial interests:** The author declares no competing financial and non-financial interests.